Embedded Human Control of Robots Using Myoelectric Interfaces

Chris Wilson Antuvan, Mark Ison, and Panagiotis Artemiadis, *Member, IEEE*

***Abstract*—Myoelectric controlled interfaces have become a research interest for use in advanced prostheses, exoskeletons, and robot teleoperation. Current research focuses on improving a user's initial performance, either by training a decoding function for a specific user or implementing "intuitive" mapping functions as decoders. However, both approaches are limiting, with the former being subject specific, and the latter task specific. This paper proposes a paradigm shift on myoelectric interfaces by embedding the human as controller of the system to be operated. Using abstract mapping functions between myoelectric activity and control actions for a task, this study shows that human subjects are able to control an artificial system with increasing efficiency by just *learning* how to control it. The method efficacy is tested by using two different control tasks and four different abstract mappings relating upper limb muscle activity to control actions for those tasks. The results show that all subjects were able to learn the mappings and improve their performance over time. More interestingly, a chronological evaluation across trials reveals that the learning curves transfer across subsequent trials having the same mapping, independent of the tasks to be executed. This implies that new muscle synergies are developed and refined relative to the mapping used by the control task, suggesting that maximal performance may be achieved by learning a constant, arbitrary mapping function rather than dynamic subject- or task-specific functions. Moreover, the results indicate that the method may extend to the neural control of any device or robot, without limitations for anthropomorphism or human-related counterparts.**

***Index Terms*—Electromyography, human-robot interaction, motor learning, myoelectric control, real-time systems.**

I. Introduction

MYOELECTRIC controlled interfaces have become a major research area in recent years due to their applications in advanced prostheses, exoskeletons, and robot teleoperation. Advances in electroencephalographic (EEG) and electromyographic (EMG) signal detection and processing have given researchers reliable and noninvasive access to brain and muscle activity, which has shifted research in prosthetics, exoskeletons, and teleoperation towards establishing a connection between electromechanical systems and humans [1]. This technology offers promise to help amputees regain independence [2]–[4], humans to perform tasks beyond their physical capabilities [5]–[7], and robotic devices and machines to be teleoperated with precision [8]–[13].

The main challenge in myoelectric controlled interfaces lies in decoding neural signals to commands capable of operating the desired application. Many decoding algorithms have been developed using machine learning techniques, but these currently suffer from subject specificity and require intense training phases before any real-time application is feasible [14]–[17]. A few other approaches have implemented simple decoders meant to be intuitive for users to control simple commands, but these intuitive mappings suffer from task specificity and assume that intuitive commands translate to maximal performance for a given task [18], [19]. In both cases, the decoders are designed to maximize the initial performance of the user, which does not take advantage of a human's natural ability to form inverse models of space [20], [21], optimize control strategies [22], [23] and learn new muscle synergies [24] while completing precise physical tasks. Thus, these approaches do not necessarily provide a foundation for maximal performance over time. Before presenting the novelty of the proposed technique, it is useful to give the definitions of two concepts that will be frequently used in the paper.

1) Control task: task to be executed by the subject using the myoelectric interface, implying both the *device* to be controlled (e.g., a robot hand) as well as its possible *functions* (e.g., open/close fingers etc.);
2) Mapping function: mathematical function that maps myoelectric activity to control actions for the task, e.g., a function that will translate myoelectric signals to opening the fingers of a robot hand.

This paper proposes a paradigm shift on myoelectric control interfaces that extends beyond using trainable decoders, by suggesting arbitrary mapping functions between the neural activity and the control actions. More specifically, this paper investigates user performance with myoelectric interfaces and arbitrary mapping functions which were neither designed for the subject nor the task. By expanding on recent conclusions that online closed loop feedback control is advantageous and effective for learning decoders in myoelectric interfaces [25]–[28], the contribution of this paper is twofold.

1) We demonstrate that a user-specific decoder is not required for myoelectric interfaces, as arbitrary mapping functions can be learned without need for intuitive mappings.
2) Evidence is provided that prior learning and muscle synergies developed from a specific mapping function are retained and can transfer to new tasks.

While Pistohl *et al.* have recently evaluated performance of proportional control of multi-fingered prostheses with respect

Manuscript received August 01, 2013; revised January 16, 2014; accepted January 19, 2014. Date of publication January 23, 2014; date of current version July 03, 2014.

The authors are with the School for Engineering of Matter, Transport and Energy, Arizona State University, Tempe, AZ 85287-6106 USA (e-mail: panagiotis.artemiadis@asu.edu).

Color versions of one or more of the figures in this paper are available online at http://ieeexplore.ieee.org.

Digital Object Identifier 10.1109/TNSRE.2014.2302212

to simple 2-D cursor controls [28], to the best of the authors' knowledge, no other study has evaluated the transfer of learning for multiple control tasks nor the performance of mapping functions with regard to myoelectric control.

Four distinct mapping functions are used to control a set of two distinct tasks, using EMG signals as commands. EMG signals are collected from two biomechanically independent pairs of antagonistic muscles to encourage flexible control of the task space [24] and avoid low-level habitual synergies that have been shown to hinder user control of the task space [29]. Evaluating user control for a given trial consisting of a single task, using a specific mapping function, provides information about learning and inferred muscle synergy development. Chronological evaluation of all trials then provides information about the influence of previous trials on performance and reveals a transfer of learning significantly dependent on the previous use of a given mapping function.

The rest of the paper is organized as follows: Section II explores related works involving decoders for myoelectric controlled interfaces. Section III details the method used for this experiment. Section IV presents the results of the experiments and supports the major findings. Finally, Section V concludes the paper with a brief discussion and summary of the contribution.

II. Related Work

Decoding neural signals has been the main research focus for improving performance of myoelectric controlled interfaces since their first implementation in the 1970s [30]. Since that time, many algorithms have been developed to train a decoder specifically for a given user. Machine learning techniques are used to develop a specific decoder based on a set of training data. Classification techniques such as neural networks [2], [31], support vector machines [12], [15], [17] and random forests [32], among others, are commonly used for a discrete set of commands. For continuous commands, black-box modeling [11] and regression methods [33] are most common. However, studies by Ajiboye *et al.* have suggested that only a sparse set of natural muscle synergies are user-independent and form a low-level basis for muscle control [34]. Moreover, the system is highly nonlinear and it is very difficult to achieve good decoding accuracy even when it is trained on a single user [35]. As a result, these machine learning techniques currently result in decoders that are highly user-specific, training intensive, and limited in accuracy, all of which hinder the general performance of myoelectric controlled interfaces.

Other decoding methods focus on providing simple, intuitive commands for using myoelectric signals to control an interface with predefined actions. Nilas *et al.* [19] created Morse code-like commands using EMG signals of two muscles to represent dots and dashes which can control primitive movements on a robot. Cipriani *et al.* [18] also used two opposing muscles to concoct higher level commands based on levels of activation. While they were able to produce encouraging results, their "intuitiveness-based" commands were task specific. The former study is only for tasks where minimal user interaction commands longer performing actions, and the latter produces only a finite set of commands for a fixed set of predefined actions. In both cases, the predefined actions limit users' ability to improve performance by learning to better control the system.

Alternatively, work has been done to investigate how well humans can learn the inverse model of a predefined decoding function. Héliot *et al.* [36] assume a model of the brain to convert firing neurons to x and y position of an end-effector for common center to reach out tasks. The algorithm consists of a decoding function, inverse model, and feedback controller. This model simulates how the brain modifies neural signals based on output error in order to develop the inverse model of the decoding function. The simulation confirms that the system is able to update the inverse model in order to minimize the error. Gage *et al.* [37] show similar results experimentally, where rats gradually learned to match target audio tones by modifying cortical neuron firing rates. Taylor *et al.* [23] explored myoelectric control with monkeys and showed how closed loop feedback improved learning and performance for cortical neuron control of a three-dimensional (3-D) cursor when compared to offline open loop learning. Mosier *et al.* [21] demonstrate that closed loop feedback allows humans to remap functional control of finger movements to efficiently control motion of a 2-D cursor. Kim *et al.* [25] confirm the importance of closed loop training in humans to obtain better performance. Chase *et al.* [26] compare performance of two decoding algorithms in open and closed-loop based control strategies. The results show significant performance differences between decoders in open loop tasks, but less difference in the online closed loop control tasks. The above studies each conclude that online closed loop control is advantageous for learning and obtaining maximal performance in myoelectric controlled interfaces.

In more closely related work, closed-loop myoelectric controlled interfaces are further investigated by Radhakrishnan *et al.* in [27] to understand human motor learning. As in [26], two decoders, classified as intuitive and nonintuitive, decode EMG signal amplitude from eight muscles to generate a 2-D cursor position. The intuitive decoder maps six of the eight muscles to a vector along the 2-D plane that is most consistent with the action on the limb when the muscle contracts. The nonintuitive decoder maps six of eight muscles randomly along equally spaced vectors in the 2-D plane. Subjects are able to learn the decoders in both experiments, with performance trends best fit by exponential decay. Additionally, the results show that the intuitive decoder helps subjects achieve better performance initially, but the nonintuitive decoder has a steeper learning rate that made performance for both decoders almost equal after 192 trials.

Pistohl *et al.* [28] compare subject performance for two different myoelectrically controlled tasks. The first task is a standard cursor control task, similar to [27]. The second uses a similar mapping function, but with removed redundancies such that each muscle operates individual fingers of a robotic hand. The mapping function is intentionally made nonintuitive to users in order to emphasize a steeper learning curve. The results show similar performance trends when given visual feedback for both cursor control and hand control, indicating that subjects are able to learn separate models to effectively reach the goal in both tasks.

This previous research has established that humans are capable of forming inverse models for various decoders when presented with closed loop feedback. Although intuitive decoders

give better initial performance, other decoders with worse initial performance are capable of higher learning rates. Further, Mussa-Ivaldi *et al.* [20] propose that the human motor system attempts to uncover the novel inverse map relating the effect of motor commands on task-relevant variables through learning. This suggests that humans, while learning to perform a task with a novel control space, tend to explore the full space in order to form a complete inverse model. De Rugy *et al.* [29] indicate limitations for discovering this inverse model when dealing with biomechanically dependent muscles. They show that habitual synergies between biomechanically dependent muscle groups controlling wrist forces make exploration of novel control spaces and corresponding new synergy formation difficult. Conversely, Nazarpour *et al.* [24] demonstrate that the use of biomechanically independent and antagonistic muscles removes this restriction and allows formation of new synergies while exploring the full task space. The study presented in this paper expands this work of understanding human motor learning by investigating the performance impact of previously learned mappings on new control tasks and interfaces using antagonistic and biomechanically independent sets of muscles to ensure proper exploration of the task space can be performed while learning.

III. Methods

A. Experimental Setup

The experiments performed in this study are designed to evaluate the effect of new control tasks with common mapping functions on human motor learning. In the experiment, wireless surface EMG electrodes (Delsys Trigno Wireless, Delsys Inc.) obtain EMG signals from four upper limb muscles of a human subject. A multifunction data acquisition card (DAQ) (USB-6343X, National Instruments) acquires and digitizes the signals for input to a custom application running on a personal computer (PC). The EMG signals are processed in real time and converted to control variables for a given task via a mapping function, and the effect is displayed to the subject for online closed-loop visual feedback. The program is written in C++ using OpenGL API [38] for the graphical display.

B. Control Tasks

The two tasks tested in these experiments are shown in Fig. 1. Task 1 is a standard center to reach out task, where the subject needs to control the center (red) circle and move it on top of one of eight possible target (green) circles as fast as possible. The eight target locations (blue circles) are symmetrically distributed around the four quadrants of the circle with respect to an origin at the center of the screen, and each quadrant represents a target area.

Task 2 consists of two rectangular objects, with a straight line bisecting one edge of each object to provide orientation, as shown in Fig. 1. The goal of the task is to control the red object by resizing and orienting it to match the stationary green one. Similarly to Task 1, there are eight possible combinations of size-orientation for the green object. Each combination maps along the control axes (see Section III-C) equivalently to the target locations in Task 1. Those eight targets are similarly grouped to four target areas equivalent to the four quadrants of a circle.

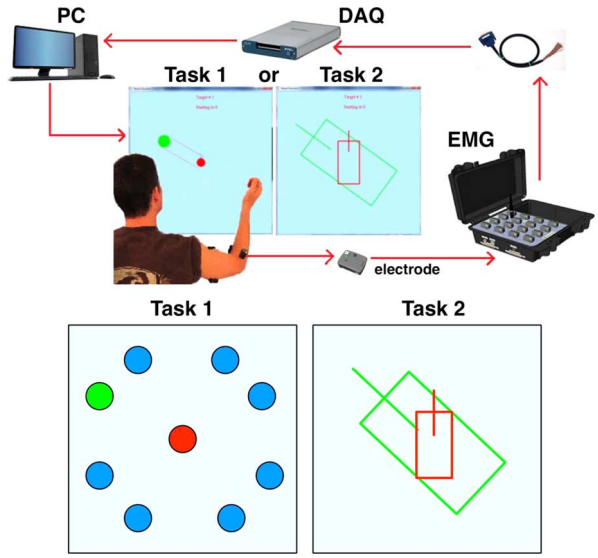

Fig. 1. Experimental setup including EMG system, DAQ, and the visual interface (top). Two tasks the subjects were asked to control using their EMG signals (bottom).

C. Mapping Functions

Myoelectric signals are obtained from four different muscles of the arm which are namely: 1) *Biceps Brachii* (BB); 2) *Triceps Brachii* (TB); 3) *Flexor Carpi Radialis* (FCR); and 4) *Extensor Carpi Ulnaris* (ECU). Following the findings from [24] that muscle synergies were quickly developed between both antagonistic and biomechanically independent muscles, and [29] that habitual synergies between biomechanically dependent muscles are difficult to alter, these four muscles were specifically chosen as two pairs of antagonistic muscles (BB/TB and FCR/ECU) which are biomechanically independent in order to enhance the potential for new synergies. The signals are sampled at 1 kHz frequency by the DAQ. The raw EMG signals undergo a preprocessing stage that is commonly used in the field of electromyography in order to compute the linear envelope of the signal [35]. The linear envelope performs full-wave rectification of the raw signals and then passes them through a low pass filter (second-order Butterworth, cutoff frequency of 8 Hz). The smoothed signal provides a reliable input signal to the mapping function for each trial.

A mapping function is implemented as 2×4 matrix which maps the 4×1 vector $\mathbf{e}$ of filtered EMG amplitudes to a 2×1 vector $\mathbf{u}$ of control outputs. Four different mapping matrices were used, shown in the following:

$$\begin{aligned}
\mathbf{u} &= \mathbf{W_i e}, \quad i = 1, 2, 3, 4 \\
\mathbf{W}_1 &= \begin{bmatrix} -1 & 1 & 0 & 0 \\ 0 & 0 & -1 & 1 \end{bmatrix} \\
\mathbf{W}_2 &= \begin{bmatrix} -0.5 & 0.5 & 0.5 & -0.5 \\ 0.5 & -0.5 & 0.5 & -0.5 \end{bmatrix} \\
\mathbf{W}_3 &= \begin{bmatrix} -0.5 & -0.5 & 0.5 & 0.5 \\ 0.5 & -0.5 & -0.5 & 0.5 \end{bmatrix} \\
\mathbf{W}_4 &= \begin{bmatrix} -0.1959 & -1 & 0.9044 & 0.2915 \\ -0.8389 & 1 & -0.6697 & 0.5086 \end{bmatrix}.
\end{aligned} \tag{1}$$

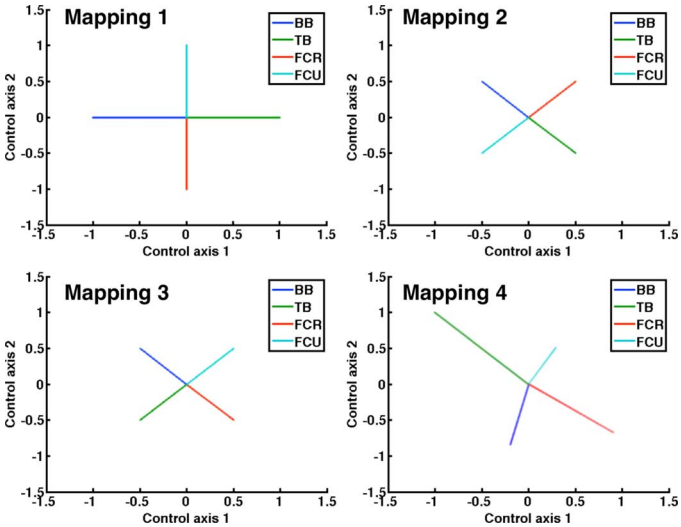

Fig. 2. Mapping of input EMG amplitudes to two output control axes using the four mappings functions defined in (1).

Each of the mapping functions transforms the EMG amplitude to control variables in a unique way that can be represented visually as vectors in the 2-D control space, as shown in Fig. 2. The control axes correspond to the velocity of the moving circle along the x (horizontal) and y (vertical) direction in the case of Task 1. For Task 2, the two control axes correspond to the angular velocity and change in size of the rectangle. An activation threshold of 0.02 mV was set for each of the muscles, so as to make sure that there is no control output when the subject is resting.

The mapping function $\mathbf{W_1}$ was designed to be the most intuitive for the subjects, according to [27]. Each set of antagonistic muscles (BB-TB and FCR-ECU) maps to only one of the two control axes required for the task. The mapping functions $\mathbf{W_2}$ and $\mathbf{W_3}$ were designed such that a combination of two muscles was required to command along one control axis direction. The mapping function $\mathbf{W_4}$ is a random matrix with arbitrary weights given to each muscle, normalized with zero mean so that there is no output at rest.

It should be noted that the subject's arm is not constrained, and muscular volume contraction (MVC) is not used to normalize the EMG signals, which differs from most other relevant studies [24], [27]–[29]. Instead of using position control with respect to MVC, subjects are free to move their arm into any configuration to fully explore each mapping and minimize the effect of potential biomechanical constraints in a given configuration. It is hypothesized that with this freedom in forming the inverse model, subjects can learn to respond and adjust appropriately to an unnormalized output when performing velocity control. Also by ignoring MVC, trends in performance over multiple days are inclusive of the performance-diminishing impact of intrasubject variability caused by sensor placement, and conclusions are robust to these sensitivities.

D. Trials

A single experiment for a subject consists of a semi-random arrangement of trials performed over a two day period. The trials are arranged so that the tasks alternate and mapping functions are not repeated until every other mapping has been seen in between, with an additional constraint that no mapping is seen twice on the same day as an attempt to minimize the feeling of familiarity for each trial. Each trial consists of a combination of task and mapping that are unknown to the subject before the trial begins. The subject is assigned to repeatedly transition a virtual object (red in Fig. 1) from a beginning state to one of eight target states (green in Fig. 1) as quickly as possible. Targets appear in a quasi-random order across trials, such that each cycle of eight targets is randomly arranged.

TABLE I
SEQUENCE OF EXPERIMENTS DONE BY SUBJECTS*

Subject 1				
Day 1	D4 I2	D3 I1	D2 I2	D1 I1
Day 2	D4 I1	D3 I2	D2 I1	D1 I2
Subject 2				
Day 1	D1 I1	D2 I2	D3 I1	D4 I2
Day 2	D1 I2	D2 I1	D3 I2	D4 I1
Subject 3				
Day 1	D4 I2	D2 I1	D1 I2	D3 I1
Day 2	D4 I1	D2 I2	D1 I1	D3 I2
Subject 4				
Day 1	D2 I1	D1 I2	D4 I1	D3 I2
Day 2	D2 I2	D1 I1	D4 I2	D3 I1
Subject 5				
Day 1	D3 I2	D1 I1	D4 I2	D2 I1
Day 2	D3 I1	D1 I2	D4 I1	D2 I2

*D# corresponds to mapping function type and I# to task type.

Five healthy subjects (23–30 years old) participated in the experiments. All subjects gave informed consent which was according to the procedures approved by the ASU IRB (Protocol: #1201007252). Each subject performed eight sets of trials (four mapping functions for each of the two types of control tasks), arranged as detailed in Table I. For each trial, subjects were given a break after 64 targets successfully reached, in order to prevent muscle fatigue. With the targets grouped into pairs to represent quadrants, each trial set of 16 repetitions per target gave 32 data points representing time taken to reach the final state for targets in a given quadrant.

IV. RESULTS

At the end of the experiments, qualitative assessment showed that all subjects considered Task 1 to be easier than Task 2 and found some mapping functions easier than others. However, none were aware that both tasks required the same input responses, though some noticed that a few of the trials required similar muscle activity to move the virtual objects.

Quantitative evaluation of learning and performance is done in three steps.

1) Confirm that learning occurred in the trials for each target area.
2) Quantify the effectiveness of prior learning transfer to subsequent trials.
3) Evaluate the overall performance of subjects when presented with each mapping function.

A. Learning

The foremost step is to identify how well subjects learn to perform the given task successfully. For this, each target area

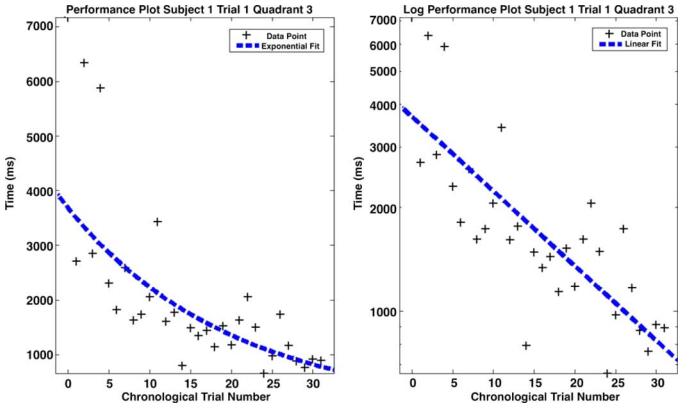

Fig. 3. Typical chronological performance trend for a trial in a given environment, both raw data and logarithmic plots.

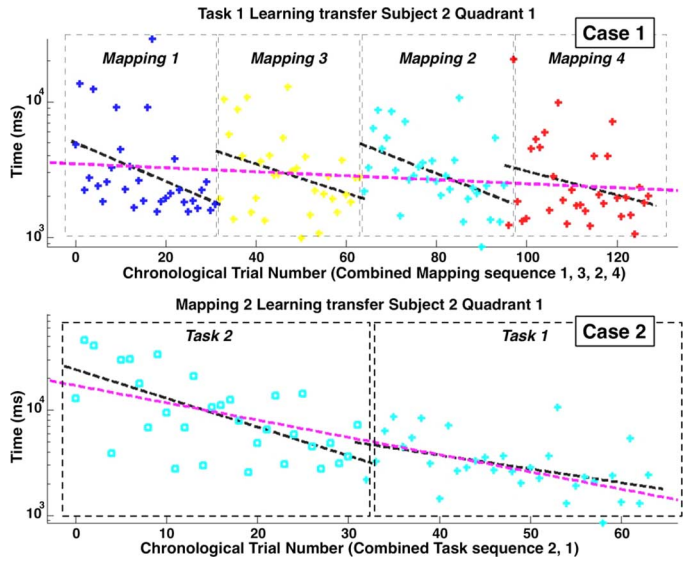

Fig. 4. Example learning transfer plots to evaluate the transition index. Top plot shows poor transfer in Case 1, while the bottom plot shows better transfer in Case 2. This is consistent with the quantitative results from the transition index.

of each trial is plotted chronologically according to the specific set of targets used in the trial. Following results from prior work [27], the general trend of learning is expected to follow an exponential decay, where initially the time required to successfully perform any task is high and it decreases exponentially towards a final steady-state value. For that reason, the data from each trial is fit to an exponential curve and the time constant of the curve gives the learning rate. The higher the time constant, the more the learning rate. To better quantify the results, the analysis here plots the data in a logarithmic scale and performs least squares regression to fit a straight line through it. In this case, steeper slope corresponds to better learning rate. Fig. 3 shows an example of a typical data pattern for one quadrant in a given trial, both with original data and the corresponding logarithmic scale. These trends are shown for all target quadrants and consistent with previous findings to imply that learning did occur within each target area.

B. Learning Transfer

The next main aspect is to compare how well learning is transferred across mapping functions for each control task (Case 1) and across control tasks for each mapping function (Case 2). This is to identify whether the subject is learning to interact with each individual control task better irrespective of the different mapping functions, or whether the subject is learning to understand the controls of each individual mapping function irrespective of the control tasks. Learning transfer can be evaluated by analyzing trials chronologically along similar task type (Case 1) or mapping function type (Case 2). For a representative subject, two plots are generated to evaluate learning transfer (see Fig. 4). The first plot (Case 1) contains the time plots in log scale, stacked side by side in the order in which a single task was performed, for each of the command sets (mapping functions). The second plot (Case 2) contains the time plot in log scale, stacked side by side in the order in which a single command set (mapping function) was used, for each of the tasks.

The important thing to observe in these figures is how smooth the transition occurs between the learning curve of one experiment to that of the next one in both cases. In order to quantify the smooth transition factor, a transition index is generated for each of the plots. In this manner, two indicators are combined to form the transition index and determine the effectiveness of learning transfer for each case.

1) Root mean squared error (RMSE) between the straight line fitted over the entire data (includes the respective trials stacked side by side) and the straight line fitted over each individual trial, as shown in Fig. 4. The lower the value the better each individual line fits the overall line.
2) Mean gap (MG) which measures the mean difference between the y coordinates of the end point of one trial's best fit line and the start point of the subsequent trial's best fit line, for all respective trials. The lower the value the more continuity between the successive trials.

Both these variables are normalized and summed for each target area to obtain the transition index, with 0 representing a perfect transfer of learning

$$TI(n,q) = \frac{\text{RMSE}(n,q)}{t} + MG(n,q) \tag{2}$$

where $TI(n,q)$ is the transition index of subject n at quadrant q, and t is the number of trials used when calculating the RMSE. This is done so as to compare the two cases with no bias for having more mapping functions than interfaces.

For each subject, the overall transition index for each control task in Case 1 and each mapping function in Case 2 is found by taking the mean over all target quadrants, as no outliers were found in any of the quadrants.

The results for Case 1 and Case 2 are listed in Tables II and III, respectively. The tables reveal that learning transfer is much more apparent when using the same mapping function with a different task (Case 2). The mean transfer over all subjects for Case 1 is 0.6833, whereas Case 2 has a significantly lower mean transfer index of 0.4959 (right-tailed two-sample t-test, $p = 0.0033$). This result suggests that the subjects were able to learn new motor controls the first time a mapping

TABLE II
TRANSITION INDEX ACROSS MAPPING FUNCTIONS FOR EACH TASK

Subject	Task 1	Task 2
1	0.5087	0.5835
2	0.8230	0.5799
3	0.6085	0.6953
4	0.8979	0.8103
5	0.5975	0.7289

TABLE III
TRANSITION INDEX ACROSS TASKS FOR EACH MAPPING FUNCTION

Subject	Mapping 1	Mapping 2	Mapping 3	Mapping 4
1	0.2824	0.2077	0.5866	0.3704
2	0.7376	0.4181	0.6795	0.4848
3	0.4986	0.9158	0.6143	0.2204
4	0.4473	0.4950	0.5498	0.3727
5	0.5118	0.2867	0.6656	0.5720

function was presented and retain this learning for at least 24 hours to be able to apply and refine the learning in a completely different task. Moreover, becoming familiar with the specific task did not help subjects achieve better performance when it was presented with a new mapping function, forcing new motor learning. This demonstrates that performance for myoelectric interfaces is therefore more dependent on a familiar mapping function than a familiar task. These results imply that a constant mapping function is better than one that is implemented for or adapts to specific tasks, and mapping functions may be generalized to new tasks while maintaining subject performance from prior training.

C. Overall Performance

Due to the significance of consistent mapping functions on learning transfer (Case 2), overall performance evaluation is quantified with a performance score incorporating learning transfer, learning rate, and end performance specifically for each mapping function. Each of these three quantities are deemed important components for evaluating how well users can interact with a given mapping function. Then, this score can be compared with initial performance, or intuitiveness of a mapping function, which is given by the start point of the best fit line for the first trial using the specified mapping. This can be visualized in Fig. 4, bottom plot. The intuitiveness is measured by the left-most point on the black line (the initial performance on the first trial). The learning rate is measured by the slope of the magenta line (best fit over all trials). The end performance is measured by the right-most point on the black line (the performance after the last trial). The transition index is as described in Section IV-B.

The performance score is measured by equally weighting end performance, learning rate, and transition index. Learning rate and transition index are considered because it is important that a mapping function should be quickly learned and easily transferred to new tasks in a dynamic environment. In order to compare the variables directly, each is normalized to have zero mean and unit standard deviation over all subjects, all mapping functions, and all quadrants. The normalized variables, summed over all quadrants, are shown for end performance and learning rate in Tables IV and V, respectively. After normalization, the three

TABLE IV
CASE 2: NORMALIZED END PERFORMANCE SCORE

Subject	Mapping 1	Mapping 2	Mapping 3	Mapping 4
1	-0.6782	-0.3930	-0.7481	-1.9281
2	0.2469	-0.3148	0.5804	-0.1250
3	-0.3136	0.9024	0.1362	-0.6530
4	0.3843	0.1242	1.2811	-0.1974
5	-0.2091	0.8640	0.3908	0.6500

TABLE V
CASE 2: NORMALIZED LEARNING RATE SCORE

Subject	Mapping 1	Mapping 2	Mapping 3	Mapping 4
1	0.6513	0.3083	1.0034	-1.8112
2	0.6167	-1.5337	0.5842	-0.6533
3	0.2851	1.2302	-1.2346	-0.0387
4	0.7753	-0.8120	0.1603	-0.3948
5	0.4854	0.0082	-0.1782	0.5481

TABLE VI
OVERALL PERFORMANCE SCORE

Subject	Mapping 1	Mapping 2	Mapping 3	Mapping 4
1	-1.5083	-2.0746	0.8711	-4.5874
2	2.5210	-2.3720	2.4398	-0.8517
3	-0.0217	5.0269	-0.2808	-2.5989
4	0.8273	-0.6849	1.8123	-1.4534
5	0.3785	-0.5722	1.4096	1.7195

TABLE VII
CASE 2: NORMALIZED INTUITIVE SCORE

Subject	Mapping 1	Mapping 2	Mapping 3	Mapping 4
1	-1.5075	-0.7908	-1.4743	0.9489
2	-0.2410	1.4684	-0.1207	0.4556
3	-0.5221	-0.5040	1.4296	-0.5755
4	-0.6857	1.0949	0.6743	0.4142
5	-0.6352	0.1570	0.5796	-0.1656

variables are simply summed to gain a final score for each subject and each mapping function. The more negative the score, the greater the performance a subject achieved for the given the mapping function, relative to the others. The final performance scores are presented in Table VI. Interestingly, the "intuitive" mapping function, $\mathbf{W}_1$ (according to Table VII), does not have the best performance score. In fact, most subjects achieve better performance with the randomized mapping function $\mathbf{W}_4$, indicating that the choice of the mapping function may not matter as much as considered in previous works. The closed loop feedback system allows users to learn the mapping and develop new muscle synergies to retain the learning and perform better when similar commands are introduced in new tasks, despite variabilities introduced through sensor placement over multiple days.

V. CONCLUSION

This paper investigates the role of mapping functions in myoelectric controlled interfaces. It is shown that subjects are not only able to learn the inverse model of arbitrary mapping functions, but more importantly are capable of generalizing this model to enhance performance on new control tasks containing similar mapping functions. Performance is determined to be more dependent on familiarity with a given mapping function than familiarity with a given control task, indicating that subjects can learn new control tasks so long as they know how

to explore the task space. This control is robust to variability caused by small changes in sensor placement that occurred while performing the experiment over multiple days. These findings imply that subjects are able to develop and refine muscle synergies for a given mapping function which enables them to explore the task space more efficiently. As mentioned in [24], the synergy development is enhanced by the choice of two pairs of antagonistic muscles, with each pair biomechanically independent. Including biomechanically dependent muscles, such as in [29], would likely hinder a subject's ability to learn these synergies due to low level mechanical restraints.

The study also reveals that the specific choice of mapping function may not be as relevant as previously emphasized in the literature. Even though mapping $\mathbf{W}_1$ appears to be the most intuitive for a majority of the subjects, the best overall performance occurs using the randomly generated mapping $\mathbf{W}_4$, and end performance for all mapping functions is more similar than the large discrepancies in initial performance. This is consistent with previous findings using closed loop feedback to learn inverse models of mapping functions [27], and another indicator of muscle synergy development to allow more efficient performance. Thus, we have proposed a myoelectric controlled interface which is not subject-specific and we also show that learning of a mapping for a particular task can still be transferred to new tasks.

The contribution of this paper is twofold: 1) it provides evidence that a user-specific decoder is not required, as long as the subject can learn a mapping function between the neural activity and the task commands and 2) it demonstrates that subjects do not only learn those mappings between their actions and the control task, but they can retain this ability and generalize it to different control tasks. These two findings support the idea of the human embedded control of devices using myoelectric interfaces, which can result in a paradigm shift in the research field of neuroprosthetics. More specifically, we have shown that humans can be trained to control different tasks by using their muscular activity directly to the control axes of the tasks (i.e., embedded control). The implications of this method are vast, since it means that humans are able to control any device, without the latter being anthropomorphic or resembling any of the human counterparts. Instead of training decoders for specific humans, humans can be trained for specific decoders, which may then generalize to a myriad of myoelectric interfaces. Tackling these problems of user specificity and extensive decoder training that can not generalize to new tasks opens new avenues and capabilities for the intelligent control of neuroprostheses.

REFERENCES

[1] J. R. Wolpaw, N. Birbaumer, D. J. McFarland, G. Pfurtscheller, and T. M. Vaughan, "Brain-computer interfaces for communication and control," *Clin. Neurophysiol.*, vol. 113, no. 6, pp. 767–791, Jun. 2002.

[2] O. Fukuda, T. Tsuji, M. Kaneko, and A. Otsuka, "A human-assisting manipulator teleoperated by EMG signals and arm motions," *IEEE Trans. Robot. Automat.*, vol. 19, no. 2, pp. 210–222, Apr. 2003.

[3] S. Bitzer and P. van der Smagt, "Learning EMG control of a robotic hand: Towards active prostheses," in *Proc. IEEE Int. Conf. Robot. and Automat. ICRA*, May 2006, pp. 2819–2823.

[4] C. Castellini, A. E. Fiorilla, and G. Sandini, "Multi-subject/daily-life activity EMG-based control of mechanical hands," *J. Neuroeng. Rehab.*, vol. 6, no. 41, 2009.

[5] L. Lucas, M. DiCicco, and Y. Matsuoka, "An EMG-controlled hand exoskeleton for natural pinching," *J. Robot. Mechatron.*, vol. 16, no. 5, Oct. 2004.

[6] P. Artemiadis and K. J. Kyriakopoulos, "EMG-based position and force estimates in coupled human-robot systems: Towards EMG controlled exoskeletons," in *Experimental Robotics*, O. Khatib, V. Kumar, and G. J. Pappas, Eds. Berlin, Germany: Springer, 2009, vol. 54, Springer Tracts in Advanced Robotics, pp. 241–250.

[7] C. Zhu, S. Shimazu, M. Yoshioka, and T. Nishikawa, "Power assistance for human elbow motion support using minimal EMG signals with admittance control," in *Proc. Int. Conf. Mechatron. Automat. (ICMA)*, Aug. 2011, pp. 276–281.

[8] T. S. Saponas, D. S. Tan, D. Morris, and R. Balakrishnan, "Demonstrating the feasibility of using forearm electromyography for musclecomputer interfaces," in *Proc. SIGCHI Conf. Human Factors in Comput. Syst.*, New York, NY, USA, 2008, CHI '08, pp. 515–524.

[9] J. Vogel, C. Castellini, and P. van der Smagt, "EMG-based teleoperation and manipulation with the DLR LWR-III," in *Proc. IEEE/RSJ Int. Conf. Intelligent Robots and Syst. (IROS)*, Sep. 2011, pp. 672–678.

[10] P. K. Artemiadis and K. J. Kyriakopoulos, "A switching regime model for the EMG-based control of a robot arm," *IEEE Trans. Syst. Man, Cybern., Part B: Cybern.*, vol. 41, no. 1, pp. 53–63, Feb. 2011.

[11] P. K. Artemiadis and K. J. Kyriakopoulos, "EMG-based teleoperation of a robot arm in planar catching movements using ARMAX model and trajectory monitoring techniques," in *Proc. IEEE Int. Conf. Robotics Automat.*, 2006, pp. 3244–3249.

[12] M. S. Erkilinc and F. Sahin, "Camera control with EMG signals using principal component analysis and support vector machines," in *Proc. IEEE Int. Syst. Conf. (SysCon)*, Apr. 2011, pp. 417–421.

[13] P. K. Artemiadis and K. J. Kyriakopoulos, "Teleoperation of a robot manipulator using EMG signals and a position tracker," in *Proc. IEEE/RSJ Int. Conf. Intelligent Robots Syst.*, Aug. 2005, pp. 1003–1008.

[14] U. Sahin and F. Sahin, "Pattern recognition with surface EMG signal based wavelet transformation," in *Proc. IEEE Syst., Man, Cybern. Conf. (SMC)*, pp. 295–300.

[15] G. Naik, D. Kumar, and Jayadeva, "Twin SVM for gesture classification using the surface electromyogram," *IEEE Trans. Inform. Technol. Biomedicine*, vol. 14, no. 2, pp. 301–308, Mar. 2010.

[16] P. K. Artemiadis, P. T. Katsiaris, and K. J. Kyriakopoulos, "A biomimetic approach to inverse kinematics for a redundant robot arm," *Autonomous Robots*, vol. 29, no. 3-4, pp. 293–308, Nov. 2010.

[17] F. Orabona, C. Castellini, B. Caputo, A. Fiorilla, and G. Sandini, "Model adaptation with least-squares SVM for adaptive hand prosthetics," in *Proc. IEEE Int. Conf. Robot. Automat.*, May 2009, pp. 2897–2903.

[18] C. Cipriani, F. Zaccone, S. Micera, and M. Carrozza, "On the shared control of an EMG-controlled prosthetic hand: Analysis of user-prosthesis interaction," *IEEE Trans. Robot.*, vol. 24, no. 1, pp. 170–184, Feb. 2008.

[19] P. Nilas, P. Rani, and N. Sarkar, "An innovative high-level human-robot interaction for disabled persons," in *Proc. IEEE Int. Conf. Robot. Automat. ICRA '04*, Apr.-May 1, 2004, vol. 3, pp. 2309–2314.

[20] F. A. Mussa-Ivaldi, M. Casadio, Z. C. Danziger, K. M. Mosier, and R. A. Scheidt, "Sensory motor remapping of space in human-machine interfaces," *Progr. Brain Res.*, vol. 191, p. 45, 2011.

[21] K. M. Mosier, R. A. Scheidt, S. Acosta, and F. A. Mussa-Ivaldi, "Remapping hand movements in a novel geometrical environment," *J. Neurophysiol.*, vol. 94, no. 6, pp. 4362–4372, Dec. 2005.

[22] J. P. Cunningham, P. Nuyujukian, V. Gilja, C. A. Chestek, S. I. Ryu, and K. V. Shenoy, "A closed-loop human simulator for investigating the role of feedback control in brain-machine interfaces," *J. Neurophysiol.*, vol. 105, no. 4, pp. 1932–1949, Apr. 2011.

[23] D. M. Taylor, S. I. H. Tillery, and A. B. Schwartz, "Direct cortical control of 3D neuroprosthetic devices," *Science*, vol. 296, pp. 1829–1832, 2002.

[24] K. Nazarpour, A. Barnard, and A. Jackson, "Flexible cortical control of task-specific muscle synergies," *J. Neurosci.*, vol. 32, no. 36, pp. 12 349–12 360, Sep. 2012.

[25] S. P. Kim, J. D. Simeral, L. R. Hochberg, J. P. Donoghue, and M. J. Black, "Neural control of computer cursor velocity by decoding motor cortical spiking activity in humans with tetraplegia," *J. Neural*, vol. 5, p. 22, 2008.
[26] S. M. Chase, A. B. Schwartz, and R. E. Kass, "Bias, optimal linear estimation, and the differences between open-loop simulation and closed-loop performance of spiking-based brain-computer interface algorithms," *Neural Networks*, vol. 22, no. 9, pp. 1203–1213, Nov. 2009.
[27] S. M. Radhakrishnan, S. N. Baker, and A. Jackson, "Learning a novel myoelectric-controlled interface task," *J. Neurophysiol.*, vol. 1, p. 47, 2008.
[28] T. Pistohl, C. Cipriani, A. Jackson, and K. Nazarpour, "Abstract and proportional myoelectric control for multi-fingered hand prostheses," *Anna. Biomed. Eng.*, vol. 41, no. 12, pp. 2687–2698, Dec. 2013.
[29] A. de Rugy, G. E. Loeb, and T. J. Carroll, "Muscle coordination is habitual rather than optimal," *J. Neurosci.*, vol. 32, no. 21, pp. 7384–7391, May 2012.
[30] D. Graupe and K. W. Cline, "Functional separation of EMG signals via ARMA identification methods for prosthesis control purposes," *IEEE Trans. Syst., Man Cybern.*, vol. SMC-5, no. 2, pp. 252–259, Mar. 1975.
[31] D. Nishikawa, W. Yu, H. Yokoi, and Y. Kakazu, "EMG prosthetic hand controller using real-time learning method," in *Proc. IEEE Int. Conf. Syst., Man, Cybern.*, 1999, vol. 1, pp. 153–158.
[32] M. V. Liarokapis, P. K. Artemiadis, P. T. Katsiaris, K. J. Kyriakopoulos, and E. S. Manolakos, "Learning human reach-to-grasp strategies: Towards EMG-based control of robotic arm-hand systems," in *Proc. IEEE Int. Conf. Robot. Automat. (ICRA)*, May 2012, pp. 2287–2292.
[33] P. K. Artemiadis and K. J. Kyriakopoulos, "An EMG-based robot control scheme robust to time-varying EMG signal features," *IEEE Trans. Inform. Technol. Biomedicine*, vol. 14, no. 3, pp. 582–588, May 2010.
[34] A. B. Ajiboye and R. F. Weir, "Muscle synergies as a predictive framework for the EMG patterns of new hand postures," *J. Neural Eng.*, vol. 6, no. 3, p. 036004, Jun. 2009.
[35] F. E. Zajac, "Muscle and tendon: Properties, models, scaling, and application to biomechanics and motor control," *Stanford Univ.*, vol. 17, p. 52, 1989.
[36] R. Héliot, K. Ganguly, J. Jimenez, and J. M. Carmena, "Learning in closed-loop brain-machine interfaces: Modeling and experimental validation," *IEEE Trans. Syst., Man, Cybern.*, vol. 40, p. 11, 2010.
[37] G. J. Gage, K. A. Ludwig, K. J. Otto, E. L. Ionides, and D. R. Kipke, "Naive coadaptive cortical control," *J. Neural Eng.*, vol. 1, p. 13, 2005.
[38] [Online]. Available: http://www.opengl.org

Chris Wilson Antuvan received the B.Tech. degree in mechanical engineering from University of Kerala, India, in 2011, and the M.S. degree in mechanical engineering from Arizona State University, Tempe, AZ, USA, in 2013.

He is a Research Assistant at the Human-Oriented Robotics and Control Lab, Arizona State University. His research interests include robotics, human machine interfaces, rehabilitation robotics, embedded controls and automation.

Mark Ison received the B.S. degree in computer science from Northwestern University, Evanston, IL, USA, in 2010, and the joint Erasmus Mundus M.S. degree in computer vision and robotics from Heriot-Watt University, Edinburgh, Scotland, Universitat de Girona, Girona, Spain, and Universite de Bourgogne, Le Creusot, France, in 2012. He is working towards the Ph.D. degree at the Human-Oriented Robotics and Control Lab, Arizona State University, Tempe, AZ, USA.

He is currently a Research Assistant at the Human-Oriented Robotics and Control Lab, Arizona State University. His research interests include rehabilitation robotics, myoelectric control systems, autonomous robotics and medical imaging.

Panagiotis Artemiadis (M'07) received the Diploma, M.S. and Ph.D. degrees in mechanical engineering from National Technical University of Athens, Greece, in 2003, 2007, and 2009, respectively.

From 2009 to 2011, he was a Postdoctoral Research Associate at the Newman Laboratory for Biomechanics and Human Rehabilitation, in the Mechanical Engineering Department, Massachusetts Institute of Technology, Boston, MA, USA. Since 2011, he has been with Arizona State University, where he is currently an Assistant Professor in the Mechanical and Aerospace Engineering Department, and Director of the Human-Oriented Robotics and Control Lab. His research interests lie in the areas of robotics, control systems, system identification, brain-machine interfaces, rehabilitation robotics, neurorobotics, orthotics, human motor control, mechatronics and human–robot interaction.